JOURNAL OF AIRCRAFT
Vol. 45, No. 4, July–August 2008

Engineering Notes

ENGINEERING NOTES are short manuscripts describing new developments or important results of a preliminary nature. These Notes should not exceed 2500 words (where a figure or table counts as 200 words). Following informal review by the Editors, they may be published within a few months of the date of receipt. Style requirements are the same as for regular contributions (see inside back cover).

Chaotic Motions of an Airfoil with Cubic Nonlinearity in Subsonic Flow

Li Daochun* and Xiang Jinwu†
Beijing University of Aeronautics and Astronautics, 100083 Beijing, People's Republic of China

DOI: 10.2514/1.32691

Introduction

FROM the first investigation in the 1950s [1], airfoil motion in subsonic flow with cubic nonlinearity has been studied by many researchers [2–9], and an excellent survey of this topic is given in [2]. Zhao and Yang [3] have detected chaos from a cubic aeroelastic system using quasi-static aerodynamics. When the unsteady aerodynamics are used, Price et al. [4] have also observed the chaotic motion with the cubic nonlinearity in pitch, and have shown that the route to chaos is period doubling. Recently, Lee and Liu [5] found that the chaotic behavior is possible with coupled cubic restoring force in pitch and plunge.

It is noted that, in the previous literature [4–9], the elastic axis was located at a quarter-chord point (the aerodynamic center), where the moment of circulatory flow becomes zero. As we know, the aerodynamic force and moment have important effects on the aeroelastic response. In this note, the case of when the moment caused by circulatory flow does not equal to zero is investigated. The bending-torsion aeroelastic equations with cubic nonlinearity in pitch have been solved using a Runge–Kutta (RK) scheme. Some interesting observations, especially a new route to chaos, are detected.

Equations of Airfoil Motion

Figure 1 gives the sketch of a two-dimensional airfoil section oscillating in pitch and plunge. The plunge deflection is denoted by h, positive in the downward direction, and α is the pitch angle about the elastic axis, positive nose-up rotation. The elastic axis is located at a distance ab from the midchord, whereas the mass center is located at a distance db from the elastic axis, where b is the semichord of the airfoil section. Both distances are positive when measured toward the trailing edge of the airfoil.

For incompressible flow, the unsteady aerodynamic force and moment are given by Fung [10] as

$$C_L(\tau) = \pi(\lambda'' - a\alpha'' + \alpha') + 2\pi\left(\alpha(0) + \lambda'(0) + \left(\frac{1}{2} - a_h\right)\alpha'(0)\right)\phi(\tau) + 2\pi\int_0^\tau \phi(\tau-\sigma)\left(\alpha'(\sigma) + \lambda''(\sigma) + \left(\frac{1}{2} - a\right)\alpha''(\sigma)\right)\mathrm{d}\sigma \quad (1)$$

$$C_M(\tau) = \pi\left(\frac{1}{2} + a\right)\left((\alpha(0) + \lambda'(0) + \left(\frac{1}{2} - a\right)\alpha'(0)\right)\phi(\tau) + \pi\left(\frac{1}{2} + a\right)\int_0^\tau \phi(\tau-\sigma)\left(\alpha'(\sigma) + \lambda''(\sigma) + \left(\frac{1}{2} - a\right)\alpha''(\sigma)\right)\mathrm{d}\sigma + \frac{\pi}{2}a(\lambda'' - a\alpha'') - \left(\frac{1}{2} - a\right)\frac{\pi}{2}\alpha' - \frac{\pi}{16}\alpha'' \quad (2)$$

Using the preceding aerodynamic force and moment, a general nondimensional form of the aeroelastic equations can be expressed as

$$m_0\lambda'' + m_1\alpha'' + m_2\lambda' + m_3\alpha' + m_4\lambda + m_5\alpha + m_6 w_1 + m_7 w_2 + m_8 w_3 + m_9 w_4 + m_{10}M_\lambda(\lambda) = 0 \quad (3)$$

$$n_0\lambda'' + n_1\alpha'' + n_2\lambda' + n_3\alpha' + n_4\lambda + n_5\alpha + n_6 w_1 + n_7 w_2 + n_8 w_3 + n_9 w_4 + n_{10}M_\alpha(\alpha) = 0 \quad (4)$$

where $w_k (k = 1, \ldots, 4)$ are new variables defined by Lee et al. [6], and m_i and n_i $(i = 1, 2, \ldots, 10)$ are functions of system parameters, the expressions of which are similar to those in [2]. For a cubic spring in the pitch degree and a linear spring in plunge, $M_\lambda(\lambda)$ and $M_\alpha(\alpha)$ in Eqs. (3) and (4) are given by

$$M_\lambda(\lambda) = \lambda, \qquad M_\alpha(\alpha) = \beta\alpha + \gamma\alpha^3 \quad (5)$$

After introducing a variable vector $\mathbf{X} = (x_1, x_2, x_3, x_4, x_5, x_6, x_7, x_8)^T$, defined as $x_1 = \alpha$, $x_2 = \alpha'$, $x_3 = \lambda$, $x_4 = \lambda'$, $x_5 = z_1$, $x_6 = z_2$, $x_8 = z_4$, $x_7 = z_3$, Eqs. (3) and (4) can be written as a set of eight first-order ordinary differential equations:

$$\mathbf{X}' = F \cdot \mathbf{X} + \mathbf{N} \quad (6)$$

where the matrix F and the vector $\mathbf{N}$ are given as follows:

$$F = \begin{bmatrix} 0 & 1 & 0 & 0 & 0 & 0 & 0 & 0 \\ f_{21} & f_{22} & f_{23} & f_{24} & f_{25} & f_{26} & f_{27} & f_{28} \\ 0 & 0 & 0 & 1 & 0 & 0 & 0 & 0 \\ f_{41} & f_{42} & f_{43} & f_{44} & f_{45} & f_{46} & f_{47} & f_{48} \\ 1 & 0 & 0 & 0 & -0.0445 & 0 & 0 & 0 \\ 1 & 0 & 0 & 0 & 0 & -0.3 & 0 & 0 \\ 0 & 0 & 1 & 0 & 0 & 0 & -0.0445 & 0 \\ 0 & 0 & 1 & 0 & 0 & 0 & 0 & -0.3 \end{bmatrix} \quad (7a)$$

Received 8 June 2007; accepted for publication 29 February 2008.

*Doctor, School of Aeronautics Science and Technology; lidc@ase.buaa.edu.cn.

†Professor, School of Aeronautics Science and Technology; xiangjwbj@sina.com.cn.

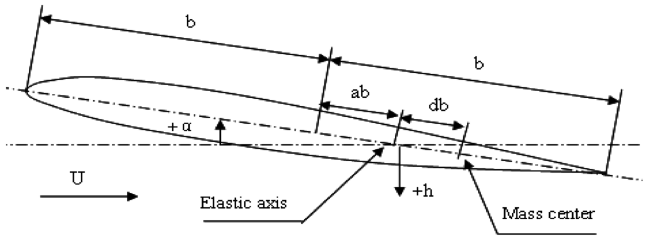

Fig. 1 Schematic of airfoil section.

$$\mathbf{N} = \begin{bmatrix} 0 \\ N_2 \\ 0 \\ N_4 \\ 0 \\ 0 \\ 0 \\ 0 \end{bmatrix} \tag{7b}$$

The elements of the matrices F and $\mathbf{N}$ can be easily obtained after some algebraic manipulations.

Results and Discussion

Equation (4) was solved numerically using an RK time-marching scheme, and, in the following example, the airfoil parameters are $r = 0.5$, $d = 0.25$, $\mu = 100$, $\varpi = 0.2$. Unlike in the literature [4–9] ($a = -0.5$), where the circulatory moment in Eq. (2) equals zero, we set $a = 0$. The nonlinear coefficients in Eq. (5) are $\beta = 0$ and $\gamma = 3$. For the initial conditions $\alpha'(0) = \lambda(0) = \lambda'(0) = 0$ and $\alpha(0) = 0.01$, a typical bifurcation diagram of the pitch response as a function of nondimensional velocity U_0 is displayed in Fig. 2a. The numerical results in the figure show the value of α when $\alpha' = 0$, and the transient responses had been damped out before the construction of the bifurcation diagram.

When $U_0 < 0.840$, the motion converges to an equilibrium point. It is interesting to note that the equilibrium points are not located at the zero position. With the velocity increasing, the distance between the equilibrium points and the $\alpha = 0$ axis increase slightly. Changing the initial conditions, the equilibrium points of pitch response will be above or below the $\alpha = 0$ axis randomly. Two examples are given in Fig. 3 for $U_0 = 0.600$. It should be pointed out that the equilibrium points of pitch response which might be above or below the $\alpha = 0$ axis are determined not only by $\alpha(0)$, but also by the other initial conditions. For example, when $\alpha(0) = \alpha'(0) = \lambda'(0) = 0$ and $\lambda(0) \neq 0$, the equilibrium points of pitch response will be above or below the $\alpha = 0$ axis randomly.

A supercritical Hopf bifurcation can be identified at $U_0 = 0.840$, approximately. Then, the system response is little-amplitude limit cycle oscillation, which can be called local motion, as it is above the $\alpha = 0$ for a whole period. From the numerical bifurcation diagram, we can see that the system's global behavior (compared with the local behavior) switch irregularly between periodic and quasi-periodic motion, which is affected by the initial conditions. As an example, a bifurcation diagram for the initial conditions $\alpha(0) = 0.1$ and $\alpha'(0) = \lambda(0) = \lambda'(0) = 0$ is given in Fig. 2b.

In the bifurcation diagram, if a very large number of points occur at one velocity, this suggests that the motion is probably chaotic. An example of this is shown in Fig. 4 for $U_0 = 0.890$, $\alpha(0) = 0.01$, and $\alpha'(0) = \lambda(0) = \lambda'(0) = 0$. It was found that, no matter how long the simulation was allowed to run, the time history in Fig. 4a never reached a steady-state condition. It was suspected that this may indicate chaos, and this was investigated by forming power spectral density of the time trace. The spectral in Fig. 4b is typical of chaotic motion, which is mainly broadband without a sharp dominant frequency peak. To add further evidence to the existence of chaos, the phase trajectory and Poincaré section were obtained. The phase trajectory shown in Fig. 4c is typical of a "two-well potential" and is indicative of chaos. In Fig. 4d, it is clear that there are an extremely large number of points in the Poincaré section, indicating nonperiodic motion. Furthermore, there is some "structure" in the Poincaré section indicating that the motion is not random but is most probably chaotic. A far more definitive method is the use of Lyapunov exponents, which give a measure of the rate of divergence or convergence of nearby orbits in phase space; a positive Lyapunov exponent indicates a chaotic system. A positive Lyapunov exponent of 0.03 was obtained, proving that the system is chaotic. For determining the chaotic region, Fig. 5 shows Lyapunov exponents for different velocities.

To understand the route to chaos, another local bifurcation diagram near the critically chaotic velocity ($0.800 < U_0 < 0.878$) for $\alpha'(0) = \lambda(0) = \lambda'(0) = 0$ and $\alpha(0) = 0.01$ is shown in Fig. 6. When U_0 comes to 0.875, a large number of points are obtained, giving what appears to be almost a vertical line on the bifurcation diagram, which indicates chaos. A positive Lyapunov exponent of 0.011 was computed, proving the existence of local chaos, the time history of

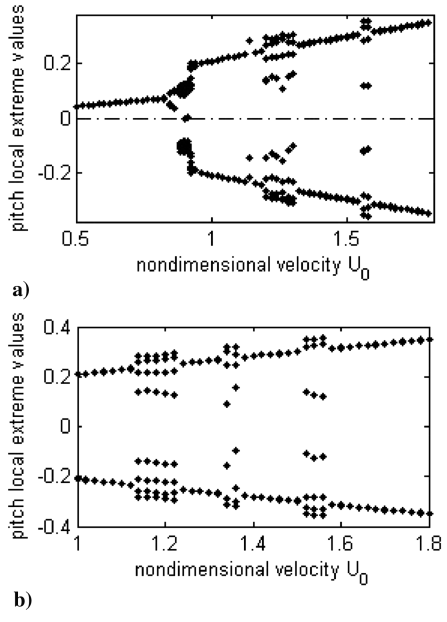

Fig. 2 Bifurcation diagrams for $\alpha'(0) = \lambda(0) = \lambda'(0) = 0$: a) $\alpha(0) = 0.01$, b) $\alpha(0) = 0.1$.

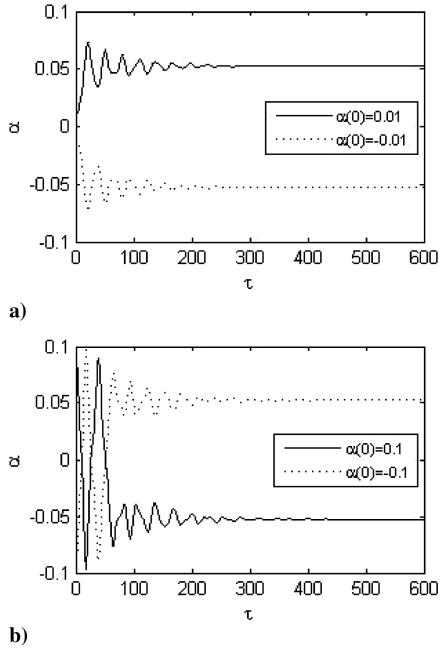

Fig. 3 Time histories for $\alpha'(0) = \lambda(0) = \lambda'(0) = 0$ and $U_0 = 0.600$.

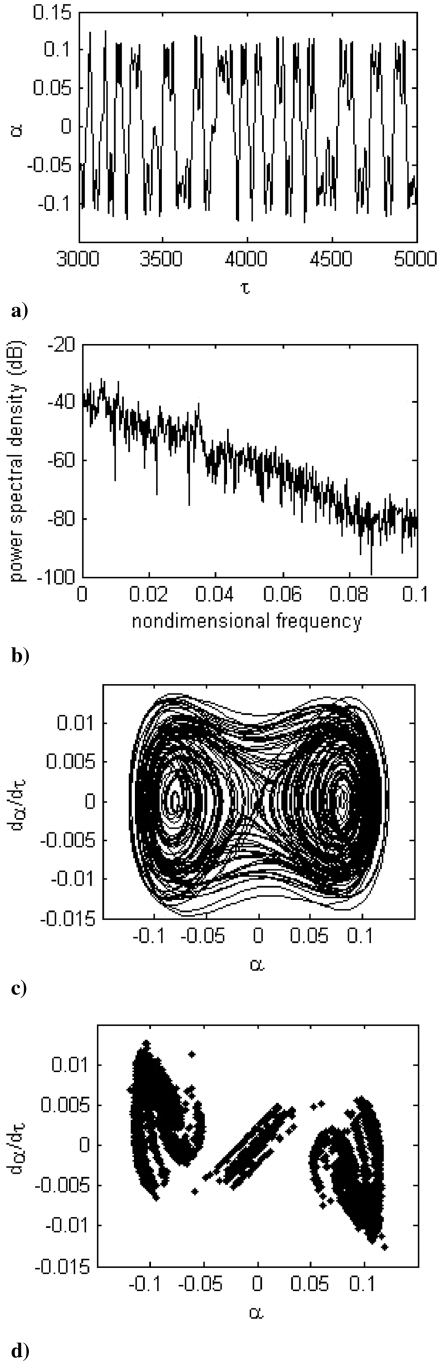

Fig. 4 Chaotic motion for $U_0 = 0.890$, $\alpha(0) = 0.01$, and $\alpha'(0) = \lambda(0) = \lambda'(0) = 0$: a) time history, b) phase trajectory, c) power spectral density, d) Poincaré section.

which is shown in Fig. 7a. When the velocity increases slightly, the system behavior expands to global motion, as shown in Fig. 7b for $U_0 = 0.877$. Now, the motion is dominant by local motions, which is above or below the $\alpha = 0$ axis. With the velocity increasing, the switching between the two types of local motion occurs more frequently until, eventually, the global chaos appeared, an example of which is given in Fig. 4. Holding on enlarging the velocity, the global chaos translates to transient chaos, an example of which is given in Fig. 7c. Then, the chaotic time is decreasing until, eventually, it becomes periodic motion.

In the examples described previously, only the pitch response was given. In fact, the plunge motion is similar to it, which can be shown in Fig. 7d. It is noted that the behaviors in pitch and plunge are "symmetric" about the equilibrium axis, namely, they always have different signs.

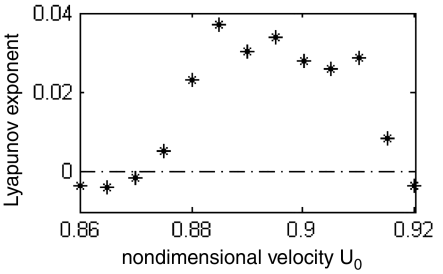

Fig. 5 Lyapunov exponent vs nondimensional velocity.

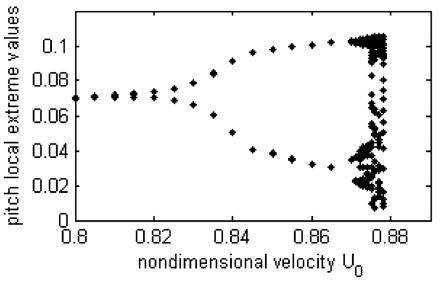

Fig. 6 Bifurcation diagram for $\alpha'(0) = \lambda(0) = \lambda'(0) = 0$ and $\alpha(0) = 0.01$.

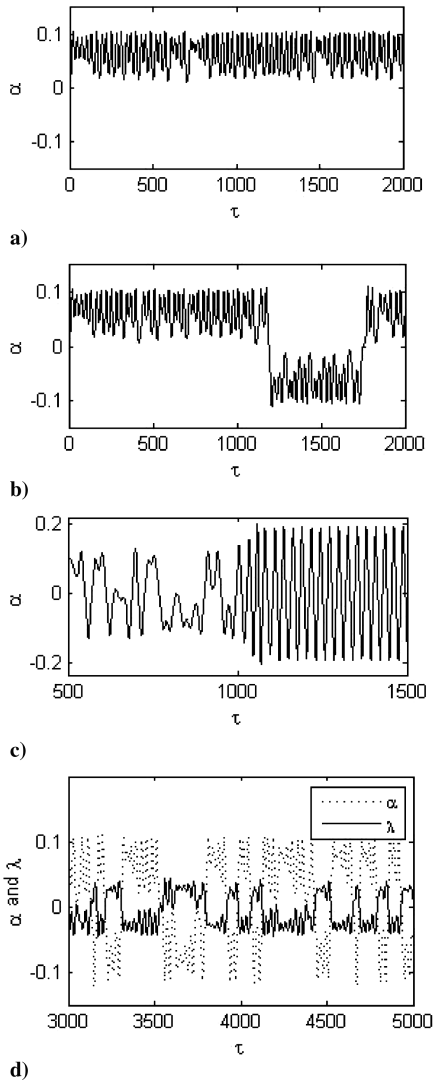

Fig. 7 Time histories for $\alpha(0) = 0.01$ and $\alpha'(0) = \lambda(0) = \lambda'(0) = 0$: a) $U_0 = 0.875$, b) $U_0 = 0.877$, c) $U_0 = 0.920$, d) $U_0 = 0.882$.

Conclusions

The aeroelastic response of a 2 degree-of-freedom airfoil placed in subsonic flow with cubic nonlinearity in pitch has been investigated using an RK method, and the nonzero circulatory moment is adopted. Different from previous results, the equilibrium point is not located at the zero point, and a mixed region of periodic and quasi-periodic motions dominates the bifurcation diagram, where the system's behavior switches irregularly between periodic and quasi-periodic motions. The effects of initial conditions on the stability boundary have been investigated by several scholars [2]. In this note, the results show that both the stable equilibrium point and the type of limit circle oscillation are also very sensitive to initial conditions. Price et al. [4] have found that there is a period-doubling route to chaos with the velocity increasing. However, local chaos is first detected in this note, and then the frequent switching between local motions leads to the global chaos. If the chaotic region is approached as velocity decreases, the route to chaos should be transient chaos.

Acknowledgments

The authors would like to acknowledge the financial support of the National Nature Science Grant of the People's Republic of China (No. 10272012) and New Century Excellent Talents at the University of the People's Republic of China (No. NCET-04-0169).

References

[1] Woolston, D. S., Runyan, H. L., and Andrews, R. E., "Investigation of Effects of Certain Types of Structural Nonlinearities on Wing and Control Surface Flutter," *Journal of the Aeronautical Sciences*, Vol. 24, No. 1, 1957, pp. 57–63.

[2] Lee, B. H. K., Price, S. J., and Wong, Y. S., "Nonlinear Aeroelastic Analysis of Airfoil: Bifurcation and Chaos," *Progress in Aerospace Sciences*, Vol. 35, No. 3, 1999, pp. 205–334. doi:10.1016/S0376-0421(98)00015-3

[3] Zhao, L. C., and Yang, Z. C., "Chaotic Motion of an Airfoil with Nonlinear Stiffness in Incompressible Flow," *Journal of Sound and Vibration*, Vol. 138, No. 2, 1990, pp. 245–254. doi:10.1016/0022-460X(90)90541-7

[4] Price, S. J., Alighanbari, H., and Lee, B. H. K., "Aeroelastic Response of a Two-Dimensional Airfoil with Bilinear and Cubic Structural Nonlinearities," *Journal of Fluids and Structures*, Vol. 9, No. 2, 1995, pp. 175–193. doi:10.1006/jfls.1995.1009

[5] Lee, B. H. K., and Liu, L., "Bifurcation Analysis of Airfoil in Subsonic Flow with Coupled Cubic Restoring Forces," *Journal of Aircraft*, Vol. 43, No. 3, 2006, pp. 652–659. doi:10.2514/1.13922

[6] Lee, B. H. K., Gong, L., and Wong, Y. S., "Analysis and Computation of Nonlinear Dynamic Response of a Two-Degree-of-Freedom System and Its Application in Aeroelasticity," *Journal of Fluids and Structures*, Vol. 11, No. 3, 1997, pp. 225–246. doi:10.1006/jfls.1996.0075

[7] Liu, L., Wong, Y. S., and Lee, B. H. K., "Application of the Center Manifold Theory in Nonlinear Aeroelasticity," *Journal of Sound and Vibration*, Vol. 234, No. 4, 2000, pp. 641–659. doi:10.1006/jsvi.1999.2895

[8] Lee, B. H. K., Liu, L., and Chung, K. W., "Airfoil Motion in Subsonic Flow with Strong Cubic Nonlinear Restoring Forces," *Journal of Sound and Vibration*, Vol. 281, Nos. 3–5, 2005, pp. 699–717. doi:10.1016/j.jsv.2004.01.034

[9] Liu, L., and Dowell, E. H., "Secondary Bifurcation of an Aeroelastic Airfoil Motion: Effect of High Harmonics," *Nonlinear Dynamics*, Vol. 37, No. 1, 2004, pp. 31–49. doi:10.1023/B:NODY.0000040033.85421.4d

[10] Fung, Y. C., *Introduction to the Theory of Aeroelasticity*, Dover, New York, 1993.